Electronic Supplementary Material (ESI) for Physical Chemistry Chemical Physics.

Supporting Information

Unusual hydroxyl migration in the fragmentation of small aminoacid dications in the gas phase.

Dariusz Grzegorz Piekarski, Rudy Delaunay, Sylvain Maclot,
Lamri Adoui, Fernando Martín, Manuel Alcamí,
Bernd A. Huber, Patrick Rousseau, Alicja Domaracka and Sergio Díaz-Tendero

April 24, 2015

1 Detailed statistics

Detailed statistics of our ab initio molecular dynamics simulations are shown in Fig. 1, 2 and 3. Total contribution of direct bond breaking in a Coulomb repulsion process is presented in Fig. 1. We can see that $C_{carboxyl} - C_\alpha$ dominates over $C_\alpha - C_\beta$ bond breaking in the whole range of the excitation energies. Fig. 2 shows the statistical results of the isomerisation of β-alanine leading to diol^{2+} (5), (4-membered ring)$^{2+}$ (8), (5-membered ring)$^{2+}$ (6) and linear $NH_3CH_2CHCOOH^{2+}$ (7)

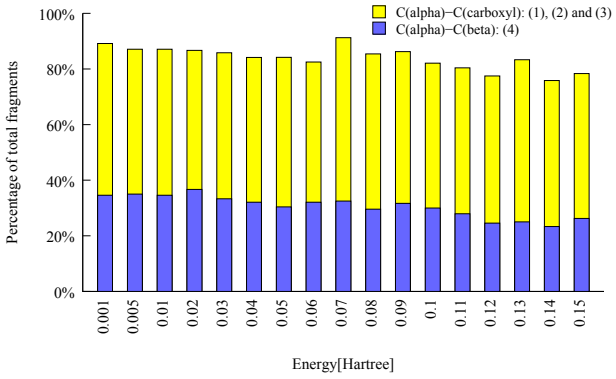

Figure 1: Statistics of the AIMD simulations showing Coulomb explosion: competition between $C_{carboxyl} - C_\alpha$: processes (1), (2), (3) and $C_\alpha - C_\beta$ bond breaking: process (4).

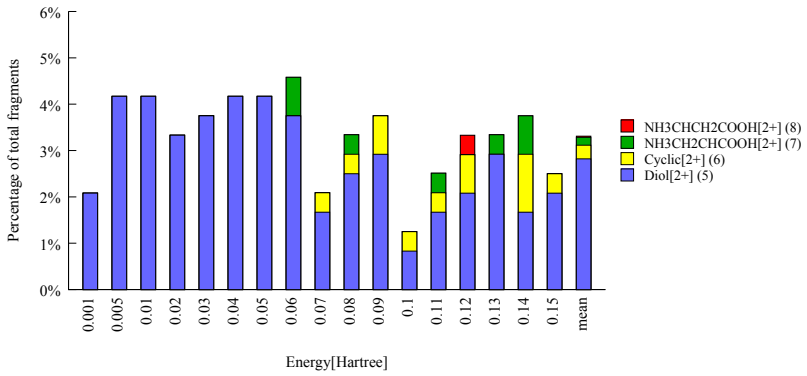

Figure 2: AIMD simulations showing isomerisation competition.

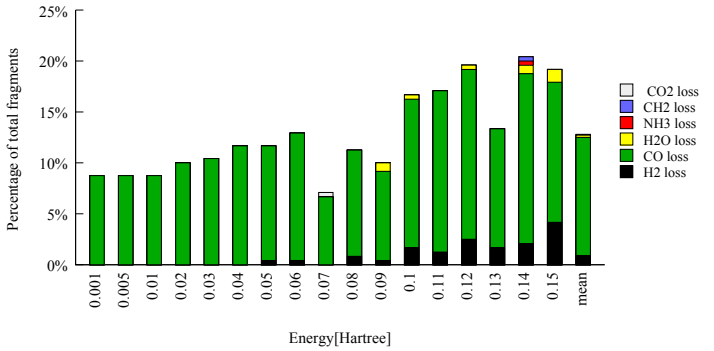

Figure 3: AIMD simulations showing combined processes competition.

as a function of the excitation energy. These channels are much less populated, about 5% (200 trajectories) of the total simulations. Isomerisation to diol^{2+}, which is the most probable isomerisation mechanism, is mainly observed for lower values of excitation energy. For larger excitation energies, we observe competition with the other processes. Fig. 3 shows combined processes. The probability of occurrence of the combined processes increases with the excitation energy. It is not surprising, as the additional excitation energy given to the vibrational degrees of freedom can induce further molecular rearrangements. Therefore, additional rearrangements appear together with the expected Coulomb repulsion, thereby decreasing the presence of repulsion processes where the excitation energy increases.

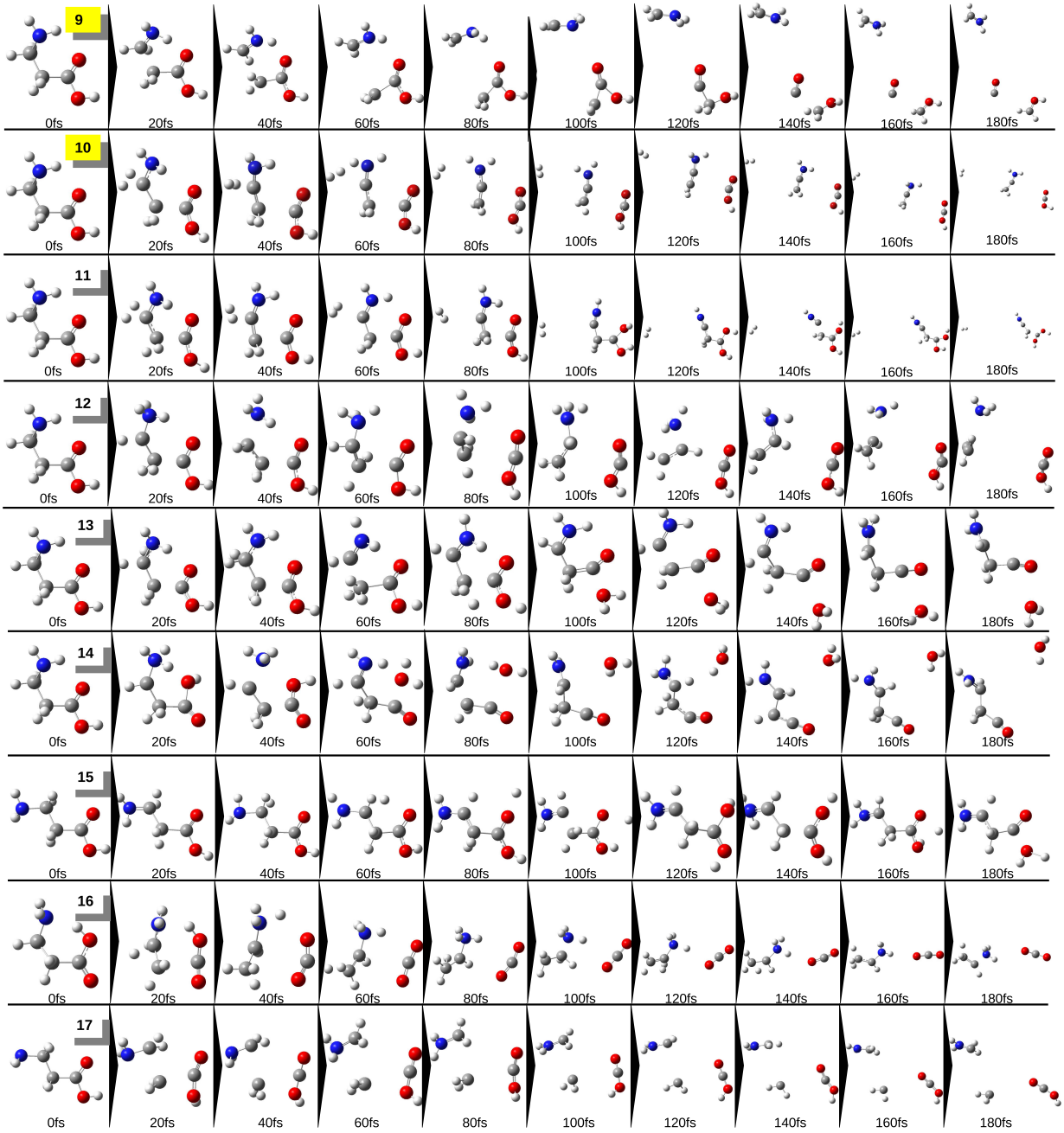

Figure 4: Snapshots of molecular dynamics simulations of a β-alanine dication giving though a combined processes: a) Coulomb explosion, isomerisation and fragmentation: (9); b) Coulomb explosion and fragmentation: (10), (17); c) fragmentation and isomerisation: (11); d) isomerisation, Coulomb explosion and fragmentation: (12); e) isomerisation and dehydration: (13), (14), (15); f) isomerisation and Coulomb explosion: (16).

2 Conformer studies

Conformers nomenclature follows the work by Sanz et al.[1] The fragmentation pattern depends on geometry of each isomer (see Fig. 5, Fig. 6 and Fig. 7) and is classified into four groups:

- $NH_2CHCH_3^+ + COOH^+$ (1): isomers a1,a2, a6, a11
- $NH_2CHCH_3^+ + COOH^+$ (1) in competition with $NH_2CH_2^+ + CH_2OH^+ + CO$ (9): isomers a3 and a12
- $NH_2CH_2^+ + CH_2COOH^+$ (4): isomers a7, a8, a9, a10
- $NH_2CH_2^+ + CH_2OH^+ + CO$ (9) in competition with $NH_2NH_2NH_2^+ + COOH^+$ (3): isomer a5

The isomer a4 can fragment in many different ways and it is not classified in any of the group above. Its geometry is very different from any other isomer and slightly similar to the geometry of a5. Indeed, conformer a5 also present a different fragmentation behavior than the others.

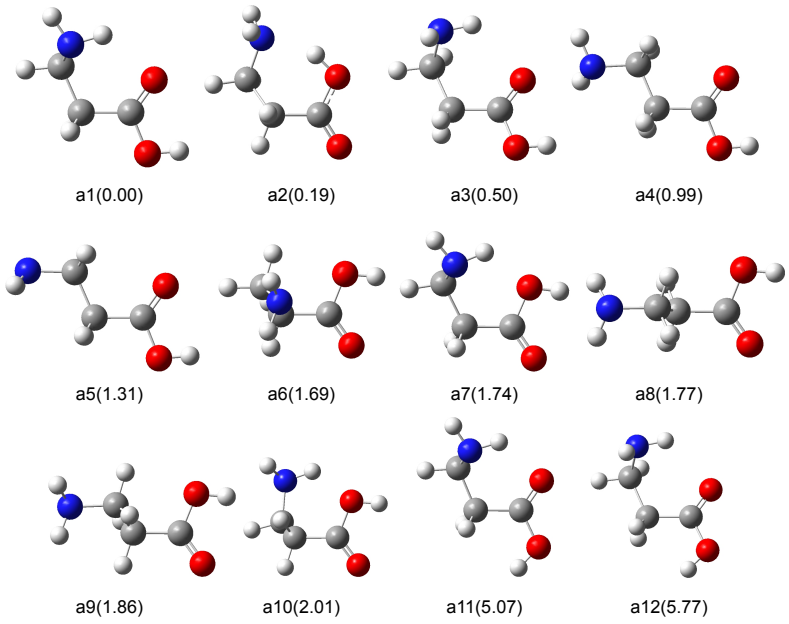

Figure 5: Geometries of the most stable 12 neutral conformers of beta-alanine. The numbers in brackets indicate the relative energy between them in kcal mol^{-1}.

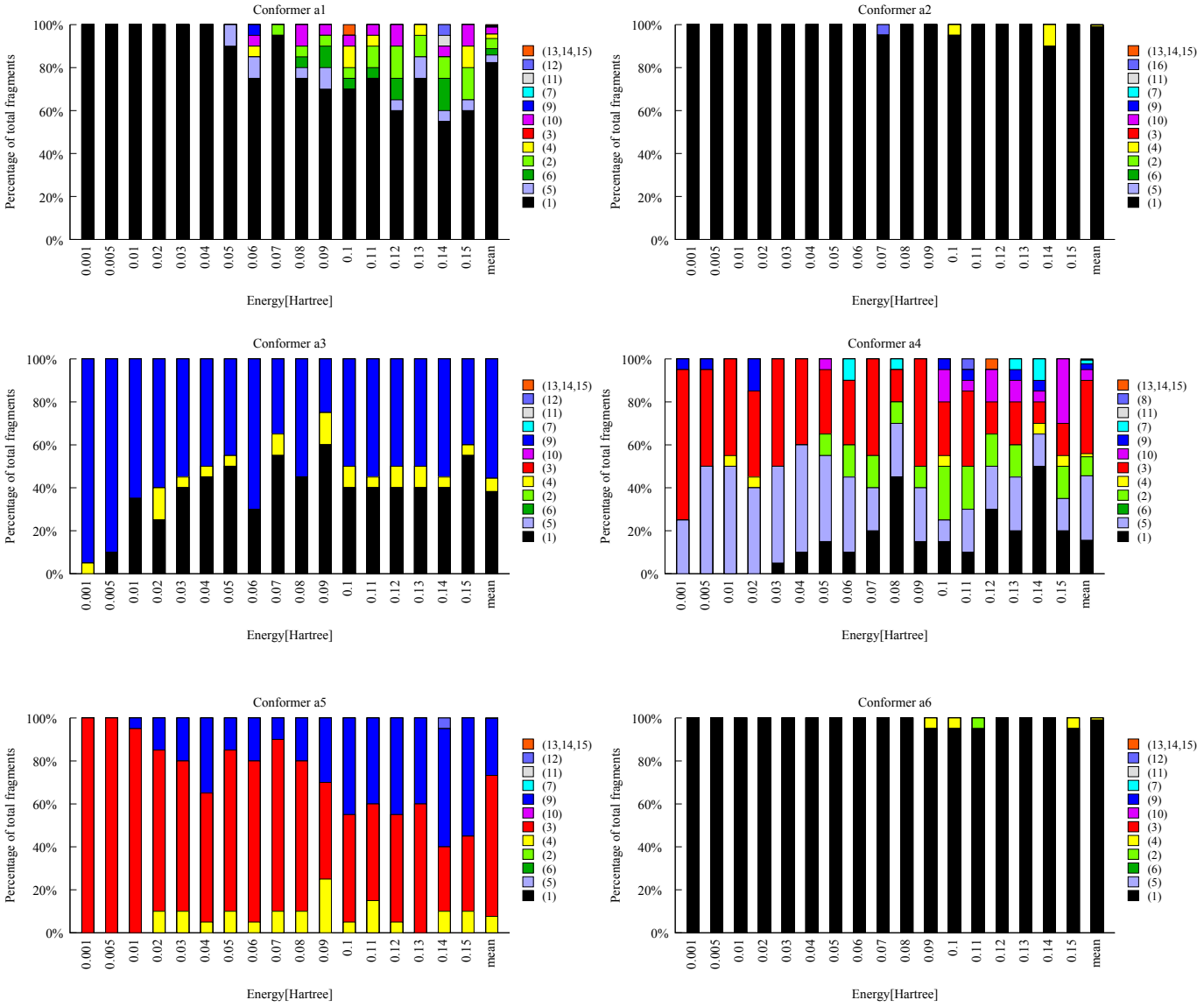

Figure 6: Ab initio molecular dynamics statistics for the six most stable conformers (a1-a6) of beta-alanine with relative energy between them 1.7 kcal mol $^{-1}$. Numbers in brackets correspond to the mechanisms defined in the article and Fig. 4.

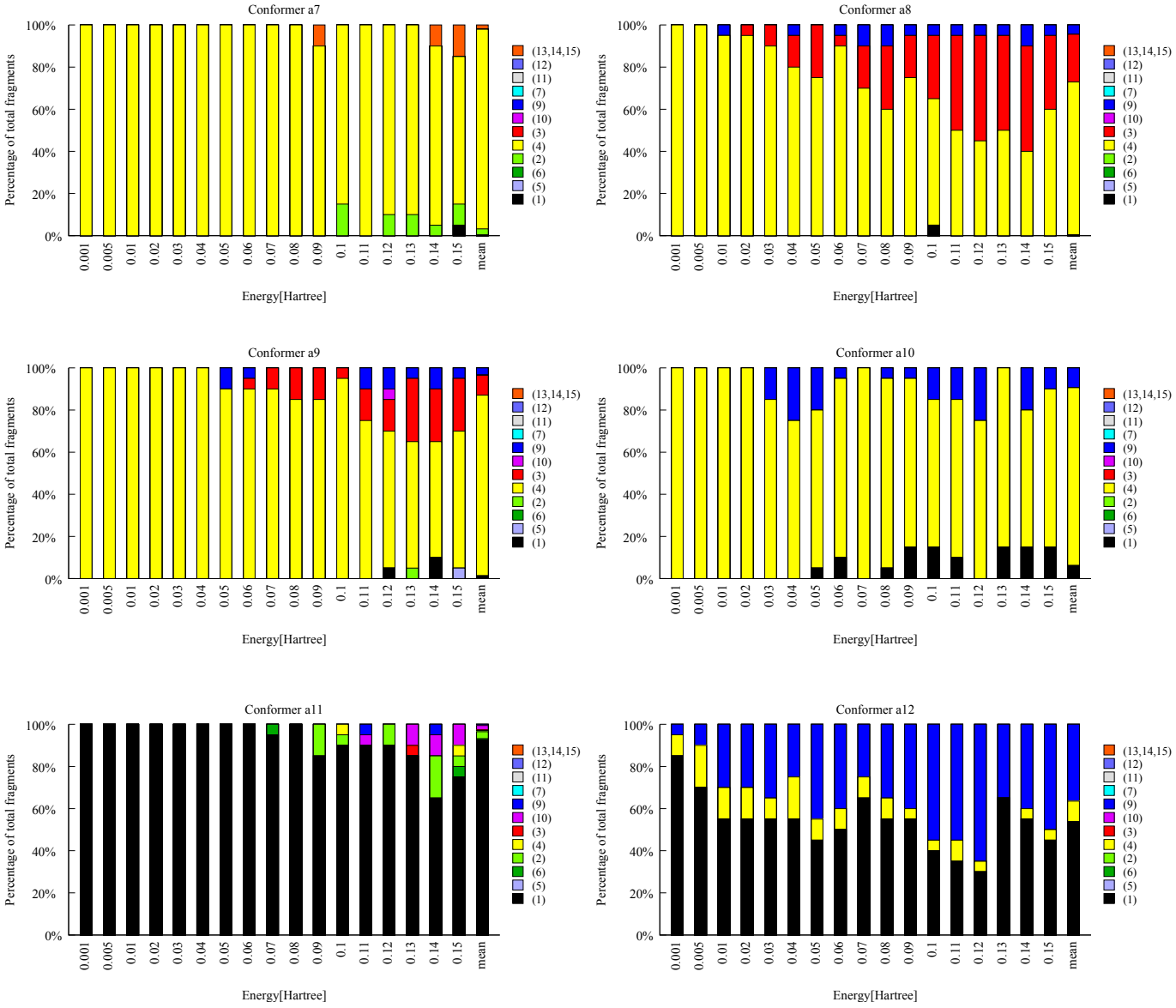

Figure 7: Ab initio molecular dynamics statistics for six conformers (a7-a12) of beta-alanine with relative energy between them 5.8 kcal mol $^{-1}$. Numbers in brackets correspond to the mechanisms defined in the article and Fig. 4.

3 Slope determination

The correlation between two charged fragments detected in coincidence gives information about the fragmentation dynamics of the doubly charged molecules. The coincidence map displays the time-of-

flight of the slower cationic fragment (TOF 2) as a function of the time-of-flight of the faster cationic fragment (TOF 1). The correlation for a given pair of charged fragments corresponds to an island on the coincidence map. The width in TOF is proportional to the momentum. The slope of islands in coincidence map can be related to the momentum of the respective cationic fragments. In a deeper analysis, the width in the TOF spectrum and the slope of one island in the coincidence map can be related to the momentum (p_i) of the respective cationic fragments:

$$S = -\frac{\Delta TOF\,2}{\Delta TOF\,1} = -\frac{p_2}{p_1} \tag{1}$$

, where $\Delta TOF\,1$ and $\Delta TOF\,2$ are the width in the TOF of the lighter and heavier fragments, respectively.

If the two cations stem from a two-body break-up or if there is a loss of a neutral product with no kinetic energy released before fragmentation of the dication into two charged species, conservation of momentum implies a slope of -1 in the respective island. In the case of a secondary decay mechanism, the island has a steeper or gentle slope. Thus, comparing the experimental slope, S_{exp}, from the shape of the island and the theoretical slope, S_{theor}, calculated from the proposed mechanisms, we can infer where the charged fragments originally come from. Experimental slopes were plotted for the most intense islands on the coincidence map. Therefore, theoretically calculated channels and experimentally measured slopes shed light on the chemical reactions and explain the behavior in the fragmentation dynamics. Comparison between the calculated slopes obtained from the computed mechanisms with the experimental measurements with the associated channels are presented in 1.

4 Summary

Fig. 8 summarizes the different studied channels, from the main pathways observed in the molecular dynamics simulations: $C_{carboxyl} - C_\alpha$ bond breaking, $C_\alpha - C_\beta$ bond breaking, H migration and OH migration; and the subsequent exploration of the potential energy surface.

Table 1: Assignation of the correlation islands corresponding to the regions of interest in the coincidence map for β-alanine dication. I_{exp} is the relative intensity as measured in the experiment. E is the highest energy barrier needed to achieve this exit channel. The number in brackets indicate the mechanism as given in the molecular dynamics simulations: (1) $NH_2CHCH_3^+ + COOH^+$, (2) $NH_3CHCH_2^+ + COOH^+$, (4) $NH_2CH_2^+ + CH_2COOH^+$, (5) $NH_2CHCH_2CO^{2+} + H_2O$, (9) $NH_2CH_2^+ + CH_2OH^+ + CO$ in the assignation column comes from $C_{carboxyl} - C_\alpha$ (1 and 2), $C_\alpha - C_\beta$ (4), H migration (5) and OH migration processes (9), respectively.

M1	M2	I_{exp}	Assignation		E	S_{theor}	S_{exp}
30	42	100	(4)$NH_2CH_2^+ + CH_2COOH^+$	$\rightarrow NH_2CH_2^+ + CH_2CO^+ + OH$	21.15	-0.71	-1.0
			$NH_2CH_2CH_2CO^{2+} + OH$	$\rightarrow NH_2CH_2^+ + CH_2CO^+ + OH$	25.70	-1.00	
30	31	80	(9)$NH_2CH_2^+ + CH_2COOH^+$	$\rightarrow NH_2CH_2^+ + CH_2OH^+ + CO$	19.55	-0.60	-
42	45	58	(1)$NH_2CHCH_3^+ + COOH^+$	$\rightarrow NH_2CCH_2^+ + H_2 + COOH^+$	20.62	-1.05	-1.1
			(1)$NH_2CHCH_3^+ + COOH^+$	$\rightarrow NHCCH_3^+ + H_2 + COOH^+$	21.33	-1.05	
28	42	47	(4)$NH_2CH_2^+ + CH_2COOH^+$	$\rightarrow NHCH^+ + H_2 + CH_2CO^+ + OH$	25.01	-0.76	-1.0
			(1)$NH_2CHCH_3^+ + COOH^+$	$\rightarrow NHCCH_3^+ + H_2 + CO^+ + OH$	25.95	-1.53	
			(5)$NH_2CHCH_2CO^{2+} + H_2O$	$\rightarrow NH_2CCH_2^+ + H + CO^+ + H_2O$	26.04	-0.98	
30	45	45	(4)$NH_2CH_2^+ + CH_2COOH^+$	$\rightarrow NH_2CH_2^+ + CH_2 + COOH^+$	22.60	-0.76	-1.4
			(1)$NH_2CHCH_3^+ + COOH^+$	$\rightarrow NH_2CH_2^+ + CH_2 + COOH^+$	22.60	-1.47	
28	45	39	(4)$NH_2CH_2^+ + CH_2COOH^+$	$\rightarrow NHCH^+ + H_2 + CH_2 + COOH^+$	24.68	-0.82	-1.4
			(1)$NH_2CHCH_3^+ + COOH^+$	$\rightarrow NHCH^+ + CH_2 + H_2 + COOH^+$	26.46	-1.57	
28	29	35	(4)$NH_2CH_2^+ + CH_2COOH^+$	$\rightarrow NHCH^+ + H_2 + CH + COH^+ + OH$	30.59	-0.53	-
28	30	31	(4)$NH_2CH_2^+ + CH_2COOH^+$	$\rightarrow NH_2CH_2^+ + CH_2OH + CO^+$	24.72	-2.11	-
43	45	30	(1)$NH_2CHCH_3^+ + COOH^+$	$\rightarrow NH_2CHCH_2^+ + H + COOH^+$	21.17	-1.02	-1.1
			(1)$NH_2CHCH_3^+ + COOH^+$	$\rightarrow NH_2CCH_3^+ + H + COOH^+$	22.01	-1.02	
			(1)$NH_2CHCH_3^+ + COOH^+$	$\rightarrow NHCHCH_3^+ + H + COOH^+$	23.91	-1.02	
29	42	29	(4)$NH_2CH_2^+ + CH_2COOH^+$	$\rightarrow NH_2CH^+ + H + CH_2CO^+ + OH$	26.14	-0.74	-1.0
			(4)$NH_2CH_2^+ + CH_2COOH^+$	$\rightarrow NHCCH_3^+ + H_2 + COH^+ + O$	28.14	-1.48	
			(4)$NH_2CH_2^+ + CH_2COOH^+$	$\rightarrow NH_2CCH_2^+ + H_2 + COH^+ + O$	28.67	-1.48	
			(5)$NH_2CHCHCOH^{2+} + H_2O$	$\rightarrow NH_2CH^+ + CHCOH^+ + H_2O$	27.05	-1.00	
			(5)$NH_2CHCH_2CO^{2+} + H_2O$	$\rightarrow NH_2CH^+ + CH_2CO^+ + H_2O$	25.45	-1.00	
			(5)$NH_2CHCH_2CO^{2+} + H_2O$	$\rightarrow NH_2CHCH^+ + COH^+ + H_2O$	21.09	-1.00	
			(5)$NH_2CHCHCOH^{2+} + H_2O$	$\rightarrow NH_2CHCH^+ + COH^+ + H_2O$	21.09	-1.00	
29	30	28	(4)$NH_2CH_2^+ + CH_2COOH^+$	$\rightarrow NH_2CH_2^+ + CH + COH^+ + OH$	28.52	-2.03	-
41	45	22	(1)$NH_2CHCH_3^+ + COOH^+$	$\rightarrow NHCCH_2^+ + H_2 + H + COOH^+$	23.06	-1.07	-1.1
			(1)$NH_2CHCH_3^+ + COOH^+$	$\rightarrow NH_2CCH^+ + H_2 + H + COH^+$	23.76	-1.07	
			(1)$NH_2CHCH_3^+ + COOH^+$	$\rightarrow NCCH_3 + H_2 + H + COOH^+$	25.84	-1.07	
14	28	21	(4)$NH_2CH_2^+ + CH_2COOH^+$	$\rightarrow NHCH^+ + H_2 + CH_2^+ + COOH$	26.32	-3.93	-
18	45	19	(2)$NH_3CHCH_2^+ + COOH^+$	$\rightarrow NH_4^+ + CHCH + COOH^+$	20.74	-2.44	-
27	45	19	(2)$NH_3CHCH_2^+ + COOH^+$	$\rightarrow NH_3 + CHCH_2^+ + COOH^+$	21.50	-1.63	-1.5
15	45	17	(1)$NH_2CHCH_3^+ + COOH^+$	$\rightarrow NH_2CH + CH_3^+ + COOH^+$	24.04	-2.93	-
28	31	14	(9)$NH_2CH_2^+ + CH_2OH^+ + CO$	$\rightarrow NHCH^+ + H_2 + CH_2OH^+ + CO$	22.01	-0.56	-
			(2)$NH_3CHCH_2^+ + COOH^+$	$\rightarrow NH_3CH_2^+ + CH + CO^+ + OH$	32.19	-1.16	

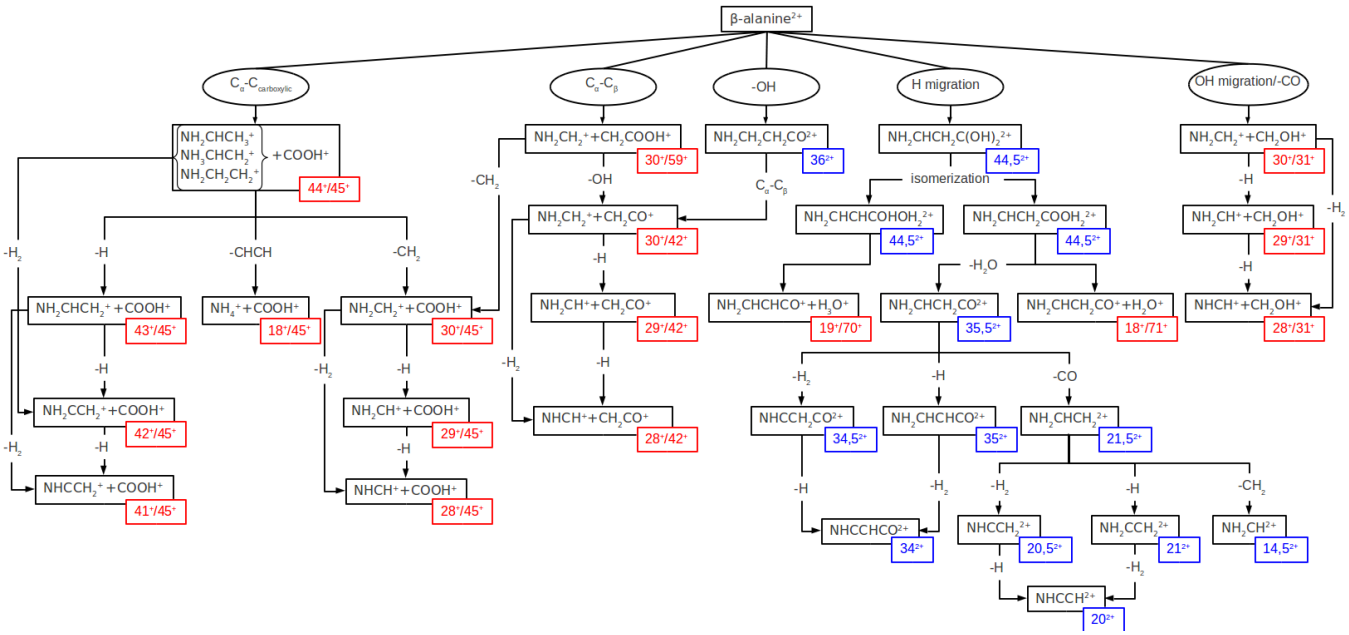

Figure 8: Schematic picture describing the five most probable fragmentation channels of doubly charged β-alanine observed in the ADMP simulations. Subsequent dissociation pathways are also presented with coincidence notation, *e.g.* $(44^+/45^+)$.

References

[1] Sanz, M. E.; Lesarri, A.; Peña, M. I.; Vaquero, V.; Cortijo, V.; López, J. C.; Alonso, J. L. *Journal of the American Chemical Society* **2006**, *128*, 3812–3817, PMID: 16536557.